Histochem Cell Biol (2014) 142:433–447
DOI 10.1007/s00418-014-1218-x

ORIGINAL PAPER

Sensory innervation of the dorsal longitudinal ligament and the meninges in the lumbar spine of the dog

Barbara Waber-Wenger · Franck Forterre · Kathrin Kuehni-Boghenbor · Renzo Danuser · Jens Volker Stein · Michael Hubert Stoffel

Accepted: 30 March 2014 / Published online: 20 April 2014

Abstract Although intervertebral disc herniation is a well-known disease in dogs, pain management for this condition has remained a challenge. The goal of the present study is to address the lack of information regarding the innervation of anatomical structures within the canine vertebral canal. Immunolabeling was performed with antibodies against protein gene product 9.5, Tuj-1 (neuron-specific class III β-tubulin), calcitonin gene-related peptide, and neuropeptide Y in combination with the lectin from *Lycopersicon esculentum* as a marker for blood vessels. Staining was indicative of both sensory and sympathetic fibers. Innervation density was the highest in lateral areas, intermediate in dorsal areas, and the lowest in ventral areas. In the dorsal longitudinal ligament (DLL), the highest innervation density was observed in the lateral regions. Innervation was lower at mid-vertebral levels than at intervertebral levels. The presence of sensory and sympathetic fibers in the canine dura and DLL suggests that pain may originate from both these structures. Due to these regional differences in sensory innervation patterns, trauma to intervertebral DLL and lateral dura is expected to be particularly painful. The results ought to provide a better basis for the assessment of medicinal and surgical procedures.

Keywords Dura · Pain · Modalities · Immunohistochemistry · Sympathetic innervation · Intervertebral disc herniation

B. Waber-Wenger · K. Kuehni-Boghenbor · M. H. Stoffel (✉)
Division of Veterinary Anatomy, Vetsuisse Faculty,
University of Bern, Länggass-Strasse 120,
POB 8466, 3001 Bern, Switzerland
e-mail: michael.stoffel@vetsuisse.unibe.ch

K. Kuehni-Boghenbor
e-mail: kathrin.kuehni@vetsuisse.unibe.ch

F. Forterre
Department of Clinical Veterinary Medicine, Vetsuisse Faculty,
University of Bern, 3001 Bern, Switzerland

R. Danuser · J. V. Stein
Theodor Kocher Institute, University of Bern, 3012 Bern, Switzerland

Introduction

Intervertebral disc (IVD) herniation is the most common spinal neurological disease in dogs. Along with neurological deficits, pain is the principal clinical sign associated with IVD herniation. Nevertheless, accurate knowledge on the innervation densities and patterns of anatomical structures within the canine vertebral canal is fragmentary. The persisting problems in pain management and the high incidence of IVD pathologies in dogs thus call for a detailed investigation of the innervation patterns within the canine lumbar spine.

Pain is the conscious perception of noxious stimuli as assimilated by nociceptors (Stoffel 2011). These receptors specifically relay information about noxious stimuli to the brain (Messlinger 1997). Back pain may arise from a number of anatomical structures (Edgar and Ghadially 1976)—such as the meninges, ligaments, joints, IVD, and nerve roots—provided that sensory innervation is present. Thus, accurate knowledge of the peripheral distribution of nociceptors is essential to understanding the origin of low-back pain.

The innervation of the spinal dura mater has been investigated in humans (Bridge 1959; Edgar and Nundy 1966; Groen et al. 1988), rats (Bridge 1959; Keller and Marfurt 1991; Ahmed et al. 1993; Kumar et al. 1996; Nakamura et al. 1996; Sekiguchi et al. 1996; Yamada et al. 1998, 2001;

Konnai et al. 2000; Saxler et al. 2008), rabbits (Kallakuri et al. 1998), dogs (Bridge 1959), and cats (Bridge 1959). In addition, some data are available on the innervation of the dorsal longitudinal ligament (DLL) in humans (Bridge 1959; Groen et al. 1988), rats (Kojima et al. 1990; Ahmed et al. 1993; Imai et al. 1995; Kumar et al. 1996; Yamada et al. 2001), rabbits (Bridge 1959; Kallakuri et al. 1998), dogs (Bridge 1959; Forsythe and Ghoshal 1984), and cats (Bridge 1959).

Nevertheless, the appraisal of the role of the dura mater in back pain has remained controversial in all species. Kumar et al. (1996) described the sensory innervation of the rat dura mater as being limited, while Bridge (1959) reported a complete absence of any intrinsic innervation of the dura mater. They concluded that the spinal pachymeninx may, at best, be marginally involved in the pathogenesis of pain. By contrast, other authors have found extensive dural innervation and have consequently established a causative link to pain (Kallakuri et al. 1998; Saxler et al. 2008). The situation regarding the specifics of the innervation pattern in the spinal dura mater is even more confusing. Whereas a predominantly ventral innervation was proposed by Groen et al. (1988) and Konnai et al. (2000), other groups reported an even fiber distribution in both the ventral and dorsal areas (Ahmed et al. 1993; Kallakuri et al. 1998; Saxler et al. 2008). With respect to current knowledge, innervation in the dura's dorsal areas seems to be less dense than in its ventral areas.

Despite the high incidence of IVD herniation in dogs, little is known about the origin of back pain in this species compared to humans and laboratory rodents. To our knowledge, only two reports concerning the presence of nerve fibers in the canine vertebral canal are available (Bridge 1959; Forsythe and Ghoshal 1984), but no information on fiber types has been published.

Although pain is generally regarded as being mediated by somatosensory neurons (Stoffel 2011), sympathetic neurotransmitters such as neuropeptide Y (NPY) (Hökfelt et al. 1986; Lundberg and Hökfelt 1986) may be involved in sensory processing and neuropathic pain (Abdulla and Smith 1999; Hökfelt et al. 2007). Furthermore, there is evidence that after spinal intervention such as laminectomy, sensory innervation increases in the rat dura (Saxler et al. 2008).

However, prior to investigating the neuronal reaction of the canine epidural tissue to painful stimuli and how sympathetic fibers may affect sensory neurons, an analysis of normal innervation patterns of these epidural structures and the demonstration of sensory and sympathetic fibers are needed.

Accordingly, a major purpose of the present immunohistochemical study was to provide new insight into the innervation of the meninges and the DLL in the normal lumbar spine of the dog with regard to nerve fiber distribution and fiber modalities.

Materials and methods

Sample collection

Samples were collected from seven adult beagles (five females, two males; all were between 4 and 6 years old) that were euthanized for reasons unrelated to lumbar spine problems.

The vertebral column was excised from T_{10} to L_7, and soft tissue was removed to expose the vertebrae. In one dog, each vertebra was bisected with an oscillating saw along the transverse plane at the mid-vertebral level, whereas soft tissues within the vertebral canal were transected with a microtome blade to avoid damage to the spinal cord and meninges. In the remaining six dogs, the vertebral arches were removed with an oscillating saw, and the spinal cord was extracted in toto together with its meningeal sleeves. In five of these dogs, the vertebral bodies with DLL from T_{10} to L_7 were partitioned at the mid-vertebral level. Vertebrae from the remaining dogs were discarded because of poor preservation.

Thus, sample collection yielded vertebral column–spinal cord (VC-SC) preparations from one dog, vertebral bodies with DLL (VB-DLL) but lacking the spinal cord from five dogs and six spinal cords in toto. All VC-SC and VB-DLL contained an intervertebral disc in the middle.

Tissue preparation

Immediately after removal, the samples were fixed in 4 % paraformaldehyde for 24 h at RT with gentle shaking. Fixation was followed by washing in 0.1 M phosphate-buffered saline (PBS; pH 7.4, Calbiochem, Canada) for several hours. The in toto spinal cords were kept in PBS until further processing.

Based on a preliminary assessment of various decalcification protocols, the VC-SC and VB-DLL preparations were decalcified in DC3 (Labonord, Templemars, France) for 5 days at RT with gentle shaking. After decalcification, samples were again washed in PBS for several hours. After slight trimming, transverse slices of approximately 0.5 cm in thickness were excised from all the samples at the level of the intervertebral discs between T_{13}/L_1 (alternatively $L_{1/2}$), $L_{2/3}$ and $L_{4/5}$ and at the mid-vertebral level of T_{13}, L_2 (alternatively L_1) and L_4. VC-SC and VB-DLL slices were freed of dispensable disc and osseous material, and the trimmed slices were transferred to cassettes for further processing.

To reduce autofluorescence, the VC-SC and VB-DLL slices and the in toto spinal cords were processed according to Alanentalo et al. (2007). In summary, the samples were dehydrated in an ascending methanol series (33, 66, 100 %), incubated in modified Dent's bleach for 24 h, washed in methanol and rehydrated in a series of Tris-buffered saline containing 0.1 % Triton X-100. The permeabilization step reported by Alanentalo et al. (2007) was omitted.

Paraffin embedding of the VC-SC and VB-DLL slices was performed according to standard protocols, and 3-µm-thick sections were cut on a rotary microtome and collected on APES-coated slides. The collection of sections from the intervertebral levels mentioned previously started at one end of the IVD, and every tenth section up to a total of 20 slices was collected for further study. In addition, approximately ten serial sections were collected from the mid-vertebral levels.

The meningeal sleeves were collected from the in toto spinal cords by carefully performing a right lateral incision with microdissection scissors. The dural sleeves were gently separated from the arachnoidal sleeves, and the preserved dura wholemounts were kept in PBS until further processing.

Immunohistochemistry

Sections

The VC-SC and VB-DLL sections were dewaxed in xylol, rehydrated in a descending series of ethanol, and subsequently washed in PBS, with all steps lasting 5 min. Residual HRP activity was quenched with 3 % H_2O_2 in PBS for 1 h before the procedure was repeated for the next primary antibody/lectin. The prescribed washing and quenching steps were performed in cuvettes to achieve the best possible results. After mounting the sections in immunostaining chambers (Coverplate TM System, Thermo Shandon, Zug, Switzerland) and washing again with PBS, a permeabilization step with 0.2 % Triton X-100 in PBS for 30 min at RT followed. Immunohistochemistry was performed with tyramide signal amplification kits (TSA Kits: T20912 Alexa 488, T20927 Alexa 350, and T20934 Alexa 568; Molecular Probes, LuBioScience, Switzerland) according to the manufacturer's instructions. For triple staining, the respective primary antibodies and lectin were mixed together for overnight incubation at 4 °C. All of the antibody–lectin combinations and dilutions used are summarized in Table 1. Dilutions were made in 1 % blocking solution, as recommended by the TSA Kit.

Washing steps after incubation of primary antibodies were executed in PBS supplemented with 0.1 % Tween. Finally, the sections were washed in PBS and mounted in Fluorescent Mounting Medium® (Dako, Baar, Switzerland).

Dura wholemounts

Immunohistochemistry with dura wholemounts from six dogs was performed according to a method described by Kallakuri et al. (1998). Samples were incubated with pertinent primary antibodies/lectin overnight at 4 °C (for combinations, see Table 1). The immunohistochemical incubation procedure was the same as for the sections, except that the washing steps were performed in 0.25 % Triton X-100 and 0.1 % Tween in PBS. For the incubation with the antibodies, the tissue was placed in sealable plastic bags but all washing steps were performed in 50-ml tubes. Prior to being mounted on slides, the dura wholemounts were longitudinally sectioned in the middle corresponding to a left

Table 1 Specifications of antibodies and lectin used

Antibody/lectin	Host	Target	Protein (µg/ml)	Combinations + Tag			Manufacturer
				I	II	III	
PGP 9.5	rb, p	Abundant cytoplasmatic neuron and neuroendocrine-cell specific protein, general neuronal marker	Not specified 1:7,500	g			RA95101, Ultraclone, Isle of Wight, UK
Tuj-1	ms, m	Neuron-specific class III-b tubulin, microtubules, general neuronal marker	2		g		MO15013, Neuromics, Edina, USA
CGRP	ms, m	C-terminal ten amino acids of CGRP, marker of sensory fibers	0.8	r		r	ab10987, abcam, Cambridge, UK
NPY	rb, p	Peptide mapping at the C-terminals of NPY, cytoplasmatic, marker of sympathetic fibers	0.2		r	g	sc-14728-R, Santa Cruz, Heidelberg, Germany
Biotinylated TL		Endothelial cells, microvasculature	10	b	b	b	L0651, Sigma, Buchs, Switzerland

Tag: g = Alexa 488 (green), r = Alexa 568 (red), b = Alexa 350 (blue)

rb rabbit, *ms* mouse, *p* polyclonal, *m* monoclonal

mid-lateral level in situ. This yielded a dorsal strip and a ventral strip which were transversely cut into pieces of appropriate sizes.

Antibody characterization

Antibodies were selected as based on their capability to differentiate between fiber types and on their applicability to canine tissue.

Information regarding all primary antibodies and the lectin used is provided in Table 1.

Protein gene product 9.5 (PGP 9.5) is an abundant neuronal cytoplasmatic protein being specific for neurons and neuroendocrine cells (Wilson et al. 1988; Day and Thompson 2010). The polyclonal rabbit–anti-human PGP 9.5 antibody used reacts with PGP 9.5 in all mammalian species tested (Jackson et al. 1985). The staining pattern in our positive controls was fully congruent with published data (Wilson et al. 1988; Willenegger et al. 2005; Peleshok and Ribeiro-da-Silva 2011).

The anti-Tuj-1 antibody (MO15013, Neuromics, Edina, USA) recognizes the neuron-specific class III β-tubulin and is regarded as a general neuronal marker as the expression of βIII-tubulin is limited to neuronal cells (Tropel et al. 2006; Higuero et al. 2010). In the present study, staining of axonal projections was in accordance with previous reports (Portmann-Lanz et al. 2010).

Neuropeptide Y is a 36 amino acid protein that consists of a polyproline stretch followed by an amphipathic α-helix. The polyclonal antibody NPY(C-20)-R: sc-14728-R (Santa Cruz Biotechnology, Inc., Santa Cruz, CA, USA) is an affinity purified antibody directed against a peptide of 15–25 amino acids mapping within the last 50 amino acids at the C-terminus of the human NPY (manufacturer's information, personal communication). NPY is present in sympathetic neurons (Lundberg and Hökfelt 1986) and co-localizes with noradrenergic nerves (Giordano 2005). Thus, NPY immunoreactivity was used to identify sympathetic neurons (Yamada et al. 2001). Staining of perivascular neuronal fibers in positive control tissue (see below) was consistent with findings in previous studies (Lundberg and Hökfelt 1986; Roudenok 2000; Giordano 2005; Arrighi et al. 2008).

The mouse monoclonal calcitonin gene-related peptide (CGRP) antibody (clone 4901, abcam, Cambridge, UK) recognizes an epitope that resides within the C-terminal ten amino acids of rat alpha CGRP. It reacts with its antigen in humans, rats, and dogs. The CGRP epitope is present in C-cells of the thyroid and in central and peripheral nerves (manufacturer's data sheet). Specificity of the staining of this anti-CGRP clone (4901) was confirmed by pre-incubating the primary antibody with pure CGRP antigen as well as with structurally unrelated peptides such as substance P, tachykinins, and others (Wong et al. 1993). CGRP immunoreactivity was demonstrated to be specific for primary sensory neurons (Rosenfeld et al. 1983). In our positive controls, the staining pattern of CGRP immunoreactivity of canine dorsal root ganglion (DRG) sections was consistent with findings reported by others (Hoover et al. 2008).

The lectin from *Lycopersicon esculentum* [Tomato Lectin (TL)] stains endothelial cells. Staining of positive control tissue with the biotinylated TL (Sigma) revealed a labeling pattern being consistent with published data (Ezaki et al. 2001).

Control experiments included the omission of the primary antibody as well as the combined omission of both the primary and secondary antibodies. In addition, an insulin antibody (mouse, monoclonal, ab6995, abcam, Cambridge, UK) and a calcitonin antibody (rabbit, polyclonal, 1720-7904, Anawa, Zürich, Switzerland) were used as irrelevant substitutes for pertinent primary antibodies. As a negative control for TL, the lectin was pre-incubated with 1 M chitin hydrolysate as a blocking sugar (SP-0090, Vector Laboratories, Burlingame, USA). Experimental and control tissues in every single experiment originated from the same animal and were processed simultaneously. Furthermore, specificity of the NPY staining was assessed by pre-absorption of the primary antibody with the NPY-antigen (sc-14728 P, Santa Cruz Biotechnology, Inc., Santa Cruz, CA, USA) for 2 h at RT. Sections of spinal cord with DRG (CGRP), adrenal gland, and sympathetic trunk (NPY), and vessel–nerve trunks (PGP 9.5, Tuj-1, and TL) were used as positive control tissues to demonstrate specific labeling of nerve or vascular structures. For control experiments, see Figs. 1 and 2.

Imaging

Sections and dura wholemounts were examined using a Zeiss AxioImager Z1 equipped with a digital high-resolution AxioCam MRm (Carl Zeiss Vision, Munich, Germany) and with the Zeiss filter sets 49, 38HE, and 43HE. Immunoreactive structures were analyzed on micrographs taken with the Mosaix Module (Axiovision Software v. 4.8.2, Carl Zeiss Vision, Munich, Germany). Images were processed uniformly as a whole with respect to brightness and contrast, and balance between the channels was adapted as appropriate. Images to be compared were processed identically.

Results

DLL paraffin sections

Nerve fibers immunoreactive to PGP 9.5, Tuj-1, CGRP, and NPY and vessels positive to TL were observed in all investigated DLL specimens from all six dogs.

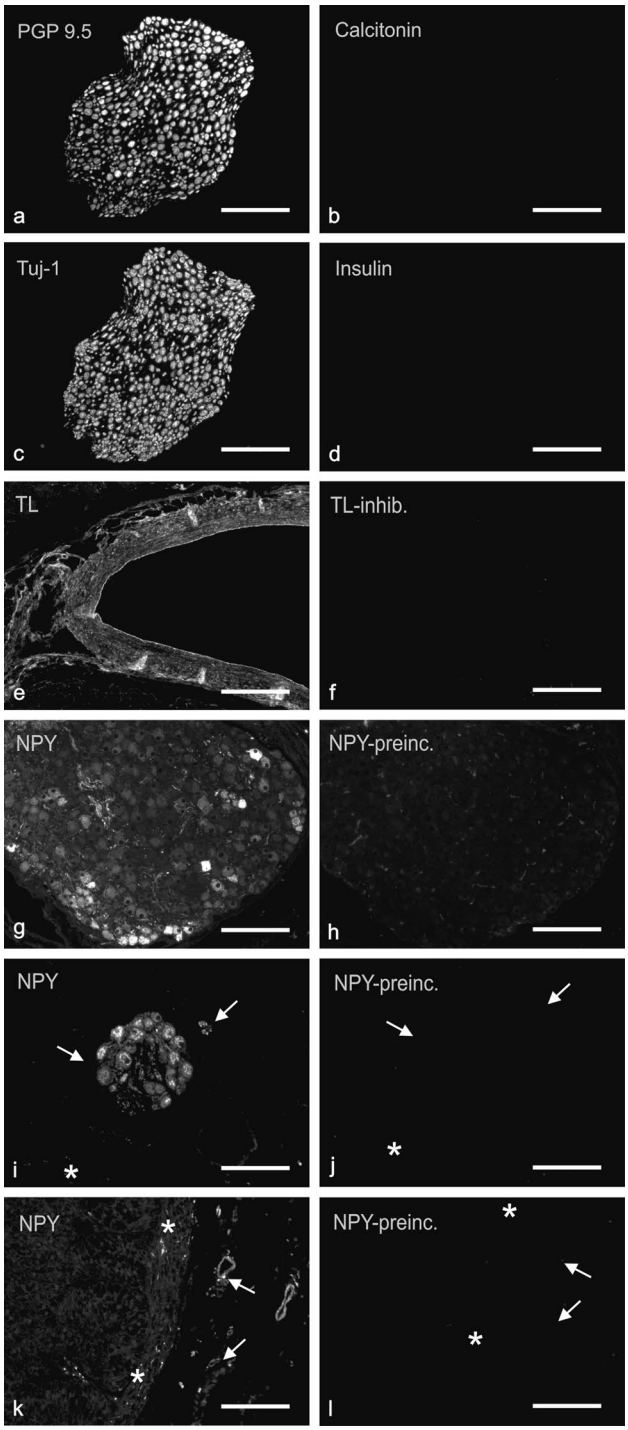

Fig. 1 Sections of canine vessel–nerve trunk (**a**–**f**), sympathetic ▶ trunk (**g**, **h**), and adrenal gland (**i**–**l**) for positive (*left column*) and negative (*right column*) control experiments. **a**, **c** Positive immunostainings of a nerve fibers with anti-PGP 9.5 and anti-Tuj-1. **b**, **d** No staining is detected in the corresponding negative controls when irrelevant substitutes for pertinent primary antibodies are used. **e** Positive staining of vessels with TL and **f** absence of staining after pre-incubation of the lectin with its blocking sugar. **g** Positive immunostaining of ganglion cells of the sympathetic trunk with anti-NPY and **h** absence of staining after pre-incubation of the primary antibody with the NPY-antigen (NPY-preinc.). **i** Positive staining of nerve cells (*arrow*) with anti-NPY next to the adrenal cortex (*asterisk*). **k** Positive staining of perivascular neuronal plexus (*arrow*) with anti-NPY next to the adrenal gland and within the cortex (*asterisks*). **j, l** Corresponding negative controls after pre-incubation of the antibody with NPY-antigen. All figures are shown in gray scale. *Scale bars* 100 µm (**a**–**d**, **i**–**l**) and 200 µm (**e**–**h**)

PGP 9.5 and Tuj-1 (general neuronal markers)

Nerve fibers immunoreactive to PGP 9.5 and Tuj-1, respectively, were detected as both running in bundles and as isolated small-diameter fibers. The longitudinal fiber orientation prevailed, while some fibers ran perpendicular to the longitudinal axis.

A similar innervation pattern was found throughout the lumbar spine. The highest innervation density occurred in the lateral regions of the DLL. Laterally, the fibers were evenly distributed throughout the deep and superficial layers (Fig. 3c), whereas medially, the fibers were almost exclusively localized to the superficial layers (Fig. 3b). Clear differences in innervation density were noted between the intervertebral and mid-vertebral levels. Compared to the mid-vertebral levels, intervertebral levels were more densely innervated, both laterally and medially. PGP 9.5- or Tuj-1-positive innervation of medial superficial layers was present in intervertebral DLL (Fig. 3a, b), whereas medial innervation was almost completely lacking at mid-vertebral levels (Fig. 3d, e).

The majority of fibers were associated with vessels, but fibers running independently were also observed. Many vessels were noted in the lateral regions at the insertions of the intervertebral DLL and were very often associated with a dense PGP 9.5- or Tuj-1-positive innervation (Fig. 3c).

CGRP (marker of sensory fibers)

Fibers immunoreactive to CGRP ran in both bundles and as isolated small-diameter fibers. The distribution pattern was similar as for the general neuronal markers. However, the density of CGRP-positive structures tended to decrease from the cranial to the caudal regions. Innervation was most dense in lateral regions. Intervertebral levels tended to be more densely innervated compared to mid-vertebral levels. In the medial superficial layers, few CGRP-positive fibers were present.

The majority of CGRP-positive fibers co-localized with PGP 9.5 and accounted for a fraction of the whole PGP 9.5-positive fiber population.

CGRP-positive fibers were partly associated with vessels but were also detected as independent fibers.

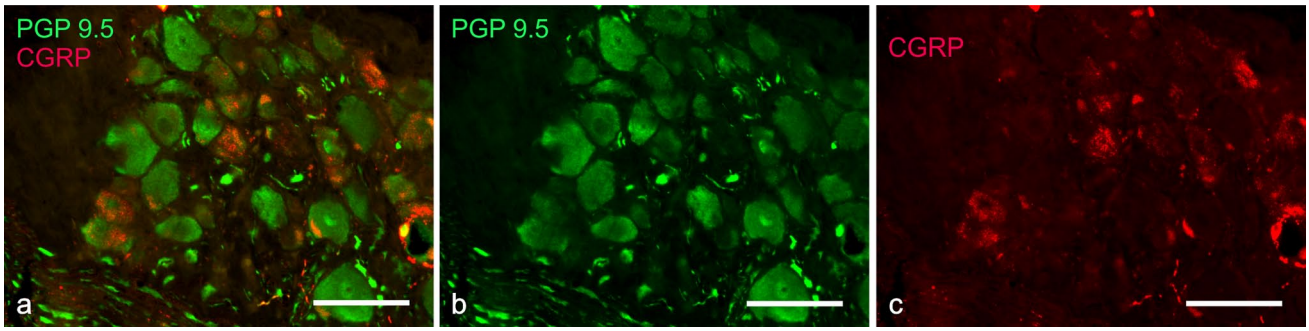

Fig. 2 Positive control for CGRP in DRG. **a** Merged channels of CGRP-positive and PGP 9.5-positive staining of ganglion cells in DRG. **b** PGP 9.5 positive ganglion cells and **c** CGRP-positive cells. *Scale bars* 100 µm (**a**–**c**)

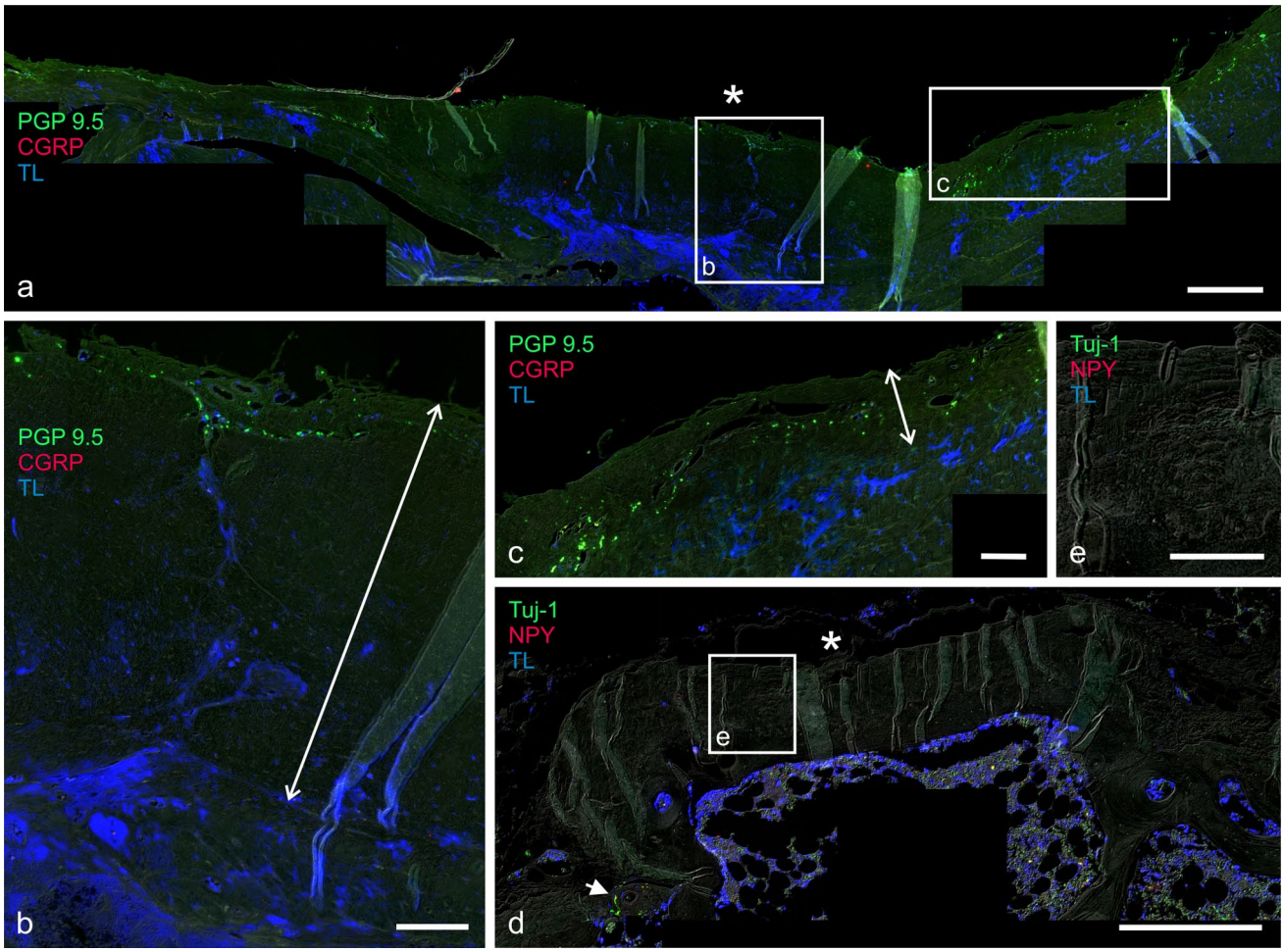

Fig. 3 Low-power micrographs of DLL cross sections at the L_4/L_5 intervertebral level (**a**) and at the L_4 mid-vertebral level (**d**), with regions of interest at higher magnifications (**b**, **c**, **e**). *Asterisks* designate the median plane (**a**, **d**), and *lines with double arrows* indicate the thickness of the DLL (**b**, **c**). **a**, **c** In lateral regions of the intervertebral DLL, PGP 9.5-positive nerve fibers are evenly distributed throughout the superficial and deep layers. **b** Innervation of medial regions of the intervertebral DLL is clearly restricted to the superficial layers. **d** Innervation density of DLL at the mid-vertebral level in lateral (*arrow*) as well as in medial (*asterisk*) regions is lower compared to intervertebral levels (**a**). **e** Medial innervation is lacking at mid-vertebral levels. **a**–**c** Combination I **d**, **e** Combination II. *Scale bars* 400 µm (**a**, **d**) and 50 µm (**b**, **c**, **e**)

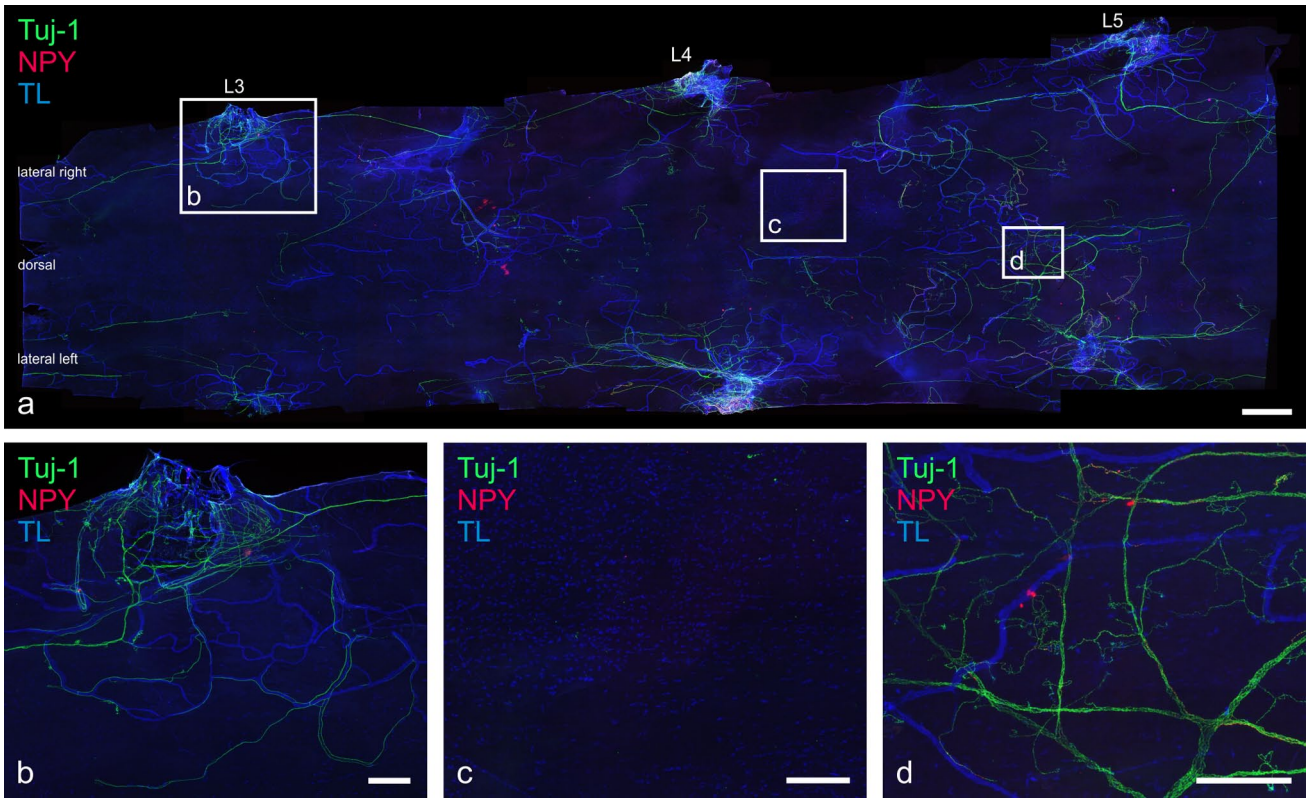

Fig. 4 Overview of the dorsal half of the dura wholemount at L_3–L_5 (**a**) and regions of interest at higher magnification (**b**–**d**). **b** High fiber density surrounding dural root sleeve (L_3). Fibers are either associated with vessels or run independently from the vascular system. **c** Areas lacking any innervation alternate with networks of high fiber density **d**. **a**–**d** Combination IV. *Scale bars* 2,000 µm (**a**) and 500 µm (**b**–**d**)

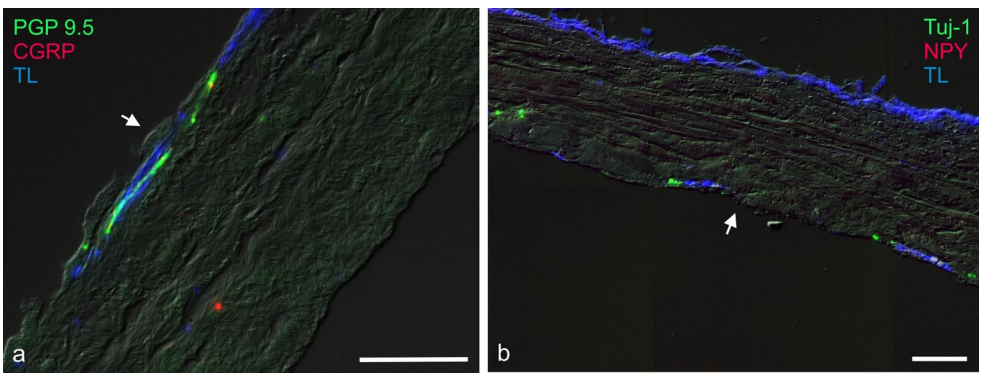

Fig. 5 Innervation of dural sheath. **a**, **b** Cross sections of the lateral dural sheath at L_4/L_5. Nerve fibers are mostly located at the outer layers of the dural sheath. *Arrows* indicate outer surface. **a** PGP 9.5-positive nerve fibers running in a transverse plane and associated with a TL-positive blood vessel. **b** Tuj-1-positive nerve fibers either associated with TL-positive vessels or running independently. **a** Combination I, **b** Combination II. *Scale bars* 50 µm

NPY (marker of sympathetic fibers)

Fibers immunoreactive to NPY ran in bundles and as isolated small fibers. The respective distribution patterns were similar to PGP 9.5 and Tuj-1. Likewise, fiber density was higher in lateral regions compared to medial DLL. Intervertebral levels also tended to contain more NPY-positive fibers both laterally and medially than at the mid-vertebral levels. Similarly, medial superficial innervation was particularly prominent in intervertebral DLL.

NPY-positive fibers co-localized with Tuj-1. They constituted a subpopulation of the Tuj-1-positive fibers. By matching the appropriate consecutive sections, not every PGP 9.5- or Tuj-1-positive fiber was either CGRP- or

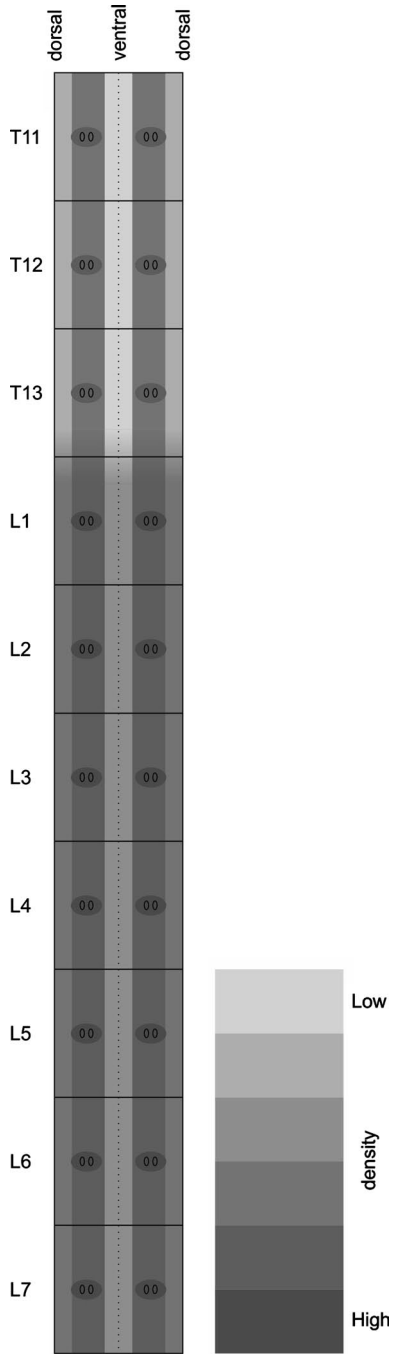

Fig. 6 The schematic drawing from spinal cord segments T11–L7 depicts the relative innervation densities in the dura mater (density increases with darkness of gray shades). In the thoracic region, density is low in dorsal and ventral areas and intermediate in the lateral areas of the dura

NPY-positive. Overall, NPY-positive fibers were more common than CGRP-positive fibers.

NPY-positive fibers were frequently associated with vessels, especially in the lateral DLL. Some fibers ran independently from vessels. NPY-positive fibers were also found in vessel walls.

Dura wholemounts

Nerve fibers immunoreactive to PGP 9.5, Tuj-1, CGRP and NPY, and vessels positive to TL were observed throughout the dura wholemount specimens.

PGP 9.5 and Tuj-1 (general neuronal markers)

Nerve fibers immunoreactive to PGP 9.5 and Tuj-1 were detected in bundles of 4–50 µm in diameter and as small isolated fibers of 0.3–4 µm in diameter, respectively (Fig. 4a). PGP 9.5- and Tuj-1-positive fibers were present throughout the full length of the lumbar dura wholemounts in the six dogs investigated.

The fibers often emerged from the root sleeves and ran both cranially and caudally along the dura. Thus, high nerve fiber density occurred near the dural root sleeves (Fig. 4b). Many fibers, especially bundles, ran in a longitudinal direction. Notably, small fibers showed an independent distribution, mainly branching in wide fiber networks (Fig. 4d).

Innervation density varied considerably along the lumbar dura, without a clear common distribution pattern. Nevertheless, overall innervation densities for PGP 9.5 and Tuj-1 tended to be the highest in lateral areas, intermediate in dorsal areas, and lowest in ventral areas. The majority of the signal was localized to the outer layers of the dural sheath (Fig. 5). Dura samples from cranial segments (from T_{11} to the middle of T_{13}/L_1) displayed few fibers in the dorsal and ventral areas and an intermediate innervation density in lateral areas. The innervation density increased caudal to L_1. This increase was more pronounced in the ventral and dorsal areas compared to lateral areas (Fig. 6). Sparsely innervated areas occurred at several spinal cord levels but varied between individual dogs (Fig. 4a, c). Highest innervation density was always observed near the dural sleeves of the spinal nerve roots and cranial to it. Small zones lacking any innervation were observed in all specimens but were irregularly distributed. By contrast, zones with a dense fiber network were established in all specimens but also lacked a general pattern (Fig. 4c, d).

PGP 9.5- and Tuj-1-positive fibers were encountered in either close association with vessels or without noticeable connection to the vascular network. Vessel-associated fibers frequently flanked the vessels on two sides. They rarely appeared to overlap the vessel over a longer distance (Fig. 7).

The endings of small-diameter fibers faded away or showed a corpuscular-like shape (Fig. 8a, b). They either ended freely in the tissue, independently from vessels, or their endings were associated with a vessel.

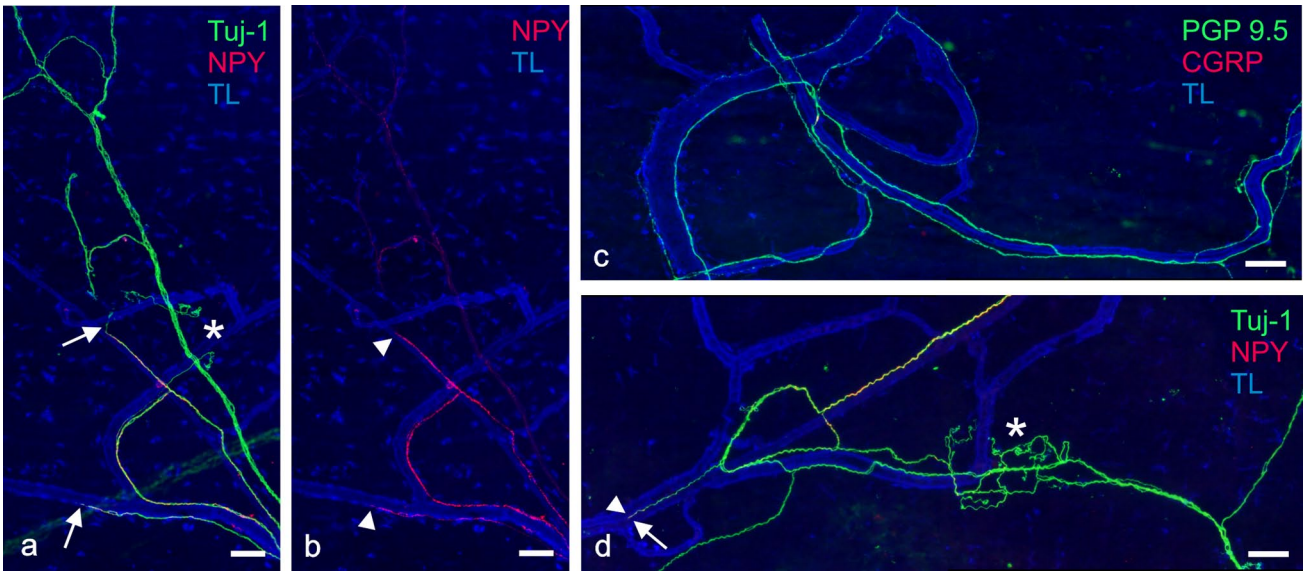

Fig. 7 Immunostaining of dura wholemounts. Nerve fibers are either related to blood vessels or run independently from the vascular system. **a**, **b** NPY-positive fibers flanking blood vessels ambilaterally (**a**: merged, **b**: NPY and TL). **c** PGP 9.5-positive nerve fibers ambilaterally running with blood vessel and crossing it. Fibers running longitudinally on top or underneath the vessel were not observed. **d** Tuj-1 positive fibers fade away (*arrow*) or show corpuscular-like endings (*asterisk*), while NPY-positive fibers always fade away (*arrowhead*) (see also **a, b**). **a**, **b**, **d** Combination IV, **c** Combination III. *Scale bars* 100 µm

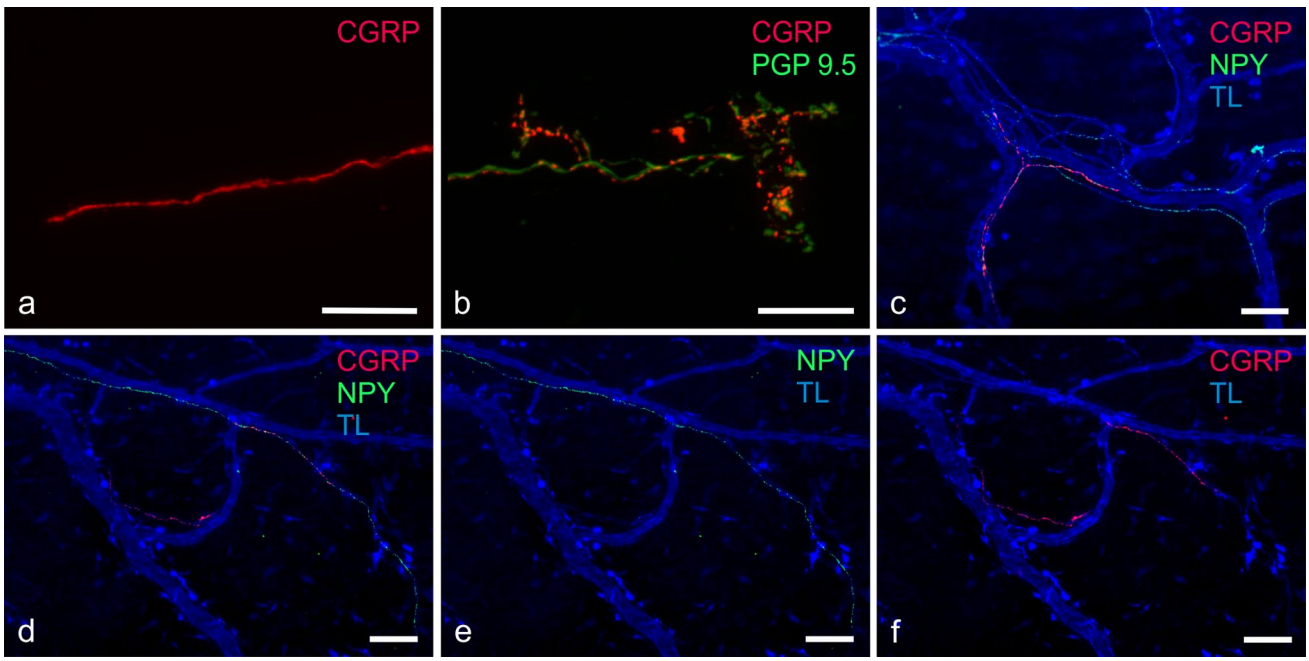

Fig. 8 Dura wholemounts (**a, b**: optical sections in ApoTome mode). **a**, **b** CGRP-positive nerve fibers either fade away (**a**) or show corpuscular-like endings (**b**). **c**–**f** NPY-positive and CGRP-positive nerve fibers running partially in close association with each other (**c**: merged, **d**: merged, **e**: NPY and TL, **f**: CGRP and TL). **a**, **c**–**f** Combination V, **b** Combination III, *Scale bars* 50 µm (**a**, **b**) and 100 µm (**c**–**f**)

CGRP (marker of sensory fibers)

CGRP-positive fibers appeared in all the specimens, running in either bundles of 4–50 µm in diameter or as small isolated fibers of 0.3–4.2 µm in diameter. The CGRP-positive fiber density was high around the dural root sleeves, due to fibers originating from the spinal nerve roots. The innervation pattern for CGRP-positive fibers was similar to

those of general neuronal markers. Innervation was sparse cranially to T_{13}/L_1 and clearly increased caudal to L_1. Cranially, CGRP-positive fibers tended to be more frequent in the lateral areas, spreading from spinal nerve sleeves. Little innervation occurred in the dorsal and ventral areas. However, the CGRP-positive fiber distribution extended all over the tissue at the caudal level. Dorsal and ventral sensory innervation density from T_{11} to L_4 varied between specimens from different individuals. The increase in innervation density caudal to L_4 was more pronounced ventrally than dorsally. Zones of very dense CGRP-positive fiber networks and zones of no CGRP-positive innervation appeared throughout the specimens but failed to follow a consistent pattern.

Most CGRP-positive fibers co-localized with PGP 9.5-positive fibers, whereas very small fibers tended to be minimal or negative for PGP 9.5. Fibers positive with CGRP accounted for a fraction of the whole PGP 9.5-positive nerve fiber population.

The majority of fibers ran by themselves, while few were associated with vessels. They faded away or ended as corpuscular-like endings (Fig. 8a, b). The fibers ended freely in the tissue or in contact with a vessel wall (Fig. 8c, f).

NPY (marker of sympathetic fibers)

Nerve fibers immunoreactive to NPY appeared in bundles of 4–50 μm in diameter and as small-diameter fibers with 0.3–2 μm in diameter. As for CGRP-positive fibers, a high proportion of NPY-positive fibers originated from the spinal nerve roots. The distribution pattern of NPY-positive fibers was similar to the spreading of the general neuronal markers, with the highest innervation density observed in the lateral areas of the dural sheath. NPY-positive innervation was sparse cranially to T_{13}/L_1, and more fibers were detected in the ventral areas than in the dorsal areas. The fiber density generally increased caudally to T_{13}/L_1. As for CGRP-positive fibers, the dorsal and ventral density of NPY-positive fibers varied among individuals up to L_4. However, a marked increase in innervation density ventrally near L_4/L_5 was noted. Zones of dense NPY-positive fiber networks and zones lacking NPY-positive innervation were occasionally noted, but no constant pattern emerged.

The majority of NPY-positive fibers co-localized with Tuj-1-positive fibers. They accounted for the majority of all Tuj-1-positive fibers. Overall, more NPY-positive fibers than CGRP-positive fibers were present. CGRP- and NPY-positive fibers ran either on their own or in close association with one another (Fig. 8c–f).

The majority of NPY-positive fibers were closely related to vessels, while some ran independently from vessels (Figs. 7b, 8d, e).

Endings of small-diameter fibers faded away, whereas NPY-positive fibers rarely showed a corpuscular-like shape in contrast to CGRP-positive fibers. Fibers either ended freely in the tissue or in contact with a vessel wall.

Discussion

The purpose of this survey was to describe the normal innervation pattern of the dura and the DLL and to assess the significance of these epidural structures in the mediation of low-back pain. The present study is the first to show the innervation pattern of the spinal dura and DLL in healthy dogs, taking into account different neuronal modalities. This report reveals accurate information on the distribution of sensory and sympathetic fibers in the canine dura and the DLL and, thus, supports the contention that pain may originate from both structures. Due to regional differences in sensory innervation patterns and densities, trauma to intervertebral DLL and lateral dura is expected to be particularly painful.

To provide a three-dimensional analysis, an effort was made to use optical projection tomography in combination with immunolabeling. However, the obtained signal intensities and specificities did not meet our expectations (data not shown). Therefore, wholemount specimens of the dura mater were investigated, and triple staining immunohistochemistry was used to relate sensory and sympathetic innervation to the vascular system. This approach yielded a comprehensive coverage of lumbar dural innervation patterns. Innervation densities in different regions were assessed on a comparative basis. Innervation of the DLL was studied on paraffin sections with identical antibodies. Based on a preliminary assessment of various antibodies and lectins, PGP 9.5, Tuj-1, CGRP, NPY, and TL turned out to be most appropriate for canine tissues.

Antibodies from different host species were selected in accordance with the requirements for triple staining. Congruency of sensory fiber labeling with CGRP and Substance P (SP) has been demonstrated in co-localization studies (Hoover et al. 2009). CGRP has been used frequently as a neuronal sensory marker (Wong et al. 1993; Imai et al. 1995; Kallakuri et al. 1998; Arrighi et al. 2008; Hoover et al. 2008, 2009). As the anti-CGRP clone 4901 from Abcam had been shown to provide specific labeling of sensory fibers in canine tissue, this antibody was favored (Hoover et al. 2008, 2009). Tyrosine hydroxylase (TH) is a well-established marker of sympathetic neurons (Ahmed et al. 1993; Imai et al. 1995; Kallakuri et al. 1998). Yet, anti-TH antibodies tested on canine adrenal gland and nerve-vessel trunk as a positive control tissue yielded unsatisfactory results in preliminary experiments. Markers detecting sympathetic neurons in canine tissue are few.

However, NPY has been shown to provide a reliable alternative to TH in rats (Ahmed et al. 1993). The demonstration of NPY-positive fibers in the DRG (Wakisaka et al. 1991) and the colocalization of NPY and CGRP in some nerve cells within the submucosal ganglia of the mouse ileum (Mongardi Fantaguzzi et al. 2009) have raised questions about the specificity of this marker for sympathetic fibers. However, Mongardi Fantaguzzi et al. 2009 reported the colocalization of NPY and CGRP signals to be very rare, and the observation of Wakisaka et al. (1991) was exclusively limited to animals that had undergone peripheral axotomy. Thus, NPY-positive fibers had never been located in purely sensory regions in healthy subjects. Similarly, NPY staining was completely absent in DRG in our control experiments. Therefore, we consider NPY to be a reliable marker for sympathetic fibers, this being in accordance with Yamada et al. (2001). To maximize the sensitivity of the testing system, tyramide-based signal amplification was used. Care was taken to ensure complete wetting of the samples in order to avoid staining artifacts.

As the samples originated exclusively from beagles, no statements regarding possible differences between breeds can be made.

Sensory innervation and pain

Primary sensory neurons are a heterogeneous group of cells which have been shown to synthesize a number of specific proteins and to exhibit typical lectin binding patterns. Correspondingly, expression of CGRP, NaV1.8, and/or the transient receptor potential vanilloid type 1 and binding of the isolectin from *Bandeiraea simplicifolia* have been used to define different though partially overlapping subgroups of sensory neurons (Andres et al. 2010). By using CGRP as the only marker, some additional nociceptors may thus have escaped detection in the present study. However, CGRP-immunoreactive cells have been shown to represent a substantial proportion of all the sensory neurons including nociceptors (Averill et al. 1995; Russo et al. 2013).

Taken together, our findings provide unequivocal evidence of putative sensory nerve fibers in both the dura mater and the DLL. As a consequence, low-back pain in the dog may arise from both these structures. Identification of prominent innervation of the DLL is in accordance with findings in rats (Kojima et al. 1990; Ahmed et al. 1993; Imai et al. 1995) and rabbits (Kallakuri et al. 1998). In the lateral DLL, nerve fibers are present in both the superficial and deep layers, whereas medial regions were only superficially innervated. This is in contrast to the situation in rabbits, in which the innervation of the DLL was reported to be evenly distributed throughout all layers (Kallakuri et al. 1998). Our findings, however, are consistent with the clinical observation that chronic IVD herniation often involves little pain (Nelson and Couto 2010), whereas in acute IVD herniation, pain is the predominant clinical sign (Simpson 1992). Acute IVD herniation often results in nuclear extrusion (Hansen Type-I) (Macias et al. 2002; Nelson and Couto 2010). Although the involvement of the DLL in IVD herniation remains unclear, empirical evidence shows that the extrusion of nuclear material entails damage to the surrounding tissues, including the DLL. By contrast, chronic IVD herniation often occurs as an annular protrusion (Hansen Type-II), and the process of prolapsing is more gradual compared to nuclear extrusions (Macias et al. 2002). As a result, the DLL is likely to be less affected and typically escapes rupture.

The innervation of the spinal dura has been a topic of controversial debate for many years. Bridge (1959) reported a complete absence of any intrinsic innervation of the canine dura mater and therefore ruled out this structure as a possible source of low-back pain. In laboratory rodents and rabbits, nerve fibers have been observed in all areas of the dura (Ahmed et al. 1993; Kallakuri et al. 1998; Saxler et al. 2008), whereas a predominantly ventral innervation is reported in humans (Groen et al. 1988) and in rats (Konnai et al. 2000). These accounts vary somewhat from our own findings, which showed intrinsic innervation in all areas of the lumbar spinal dura and revealed the overall innervation density to be highest in the lateral areas, intermediate in the dorsal areas, and lowest in the ventral areas (Fig. 6).

Likewise, controversial opinions have been proposed concerning the distribution of sensory fibers in the dura. In rats, a sparse innervation with CGRP- and substance P-positive fibers was reported in a narrow ventral strip (Kumar et al. 1996), whereas other groups observed a sensory innervation in both the ventral area and, to a lesser extent, the dorsal areas in rabbits (Kallakuri et al. 1998) and rats (Saxler et al. 2008). The present study shows CGRP-positive sensory fibers to be present in the ventral, dorsal, and lateral areas, although fiber densities in the lumbar dura were variable. As a consequence of these regional differences in sensory innervation patterns, trauma to the lateral dura, especially if caudal to T13/L1, is likely to be particularly painful compared to other regions (Fig. 6).

Furthermore, varying zones of very dense dural sensory fiber networks as well as zones without any innervation occurred throughout the specimens. It is known from humans that neurological pathologies may remain asymptomatic despite morphological evidence of IVD herniation (Boden et al. 1990). Irregular innervation patterns provide a plausible explanation for this observation and may also account for interindividual differences in pain perception in dogs.

Labeling was the most prominent in the outer layers of the dural sheath, thus making the dura especially susceptible to any extrinsic impairment.

The endings of CGRP-positive nerve fibers either faded away or were corpuscular (Fig. 8a, b). Faded nerve fibers are the morphological correlates of nociceptors (Messlinger 1997). This is consistent with the contention of a nociceptive innervation of the lumbar dura mater in the dog. Corpuscular-like endings resemble Ruffini corpuscles and are usually considered to act as mechanoreceptors (Halata 1977) and stretch receptors (Kannari et al. 1991). However, they have also been reported to be present in the dura mater encephali of the rat (Andres et al. 1987).

Surgical treatment

Various surgical treatments have been used for thoracolumbar IVD herniation in dogs: dorsal laminectomy, pediculectomy, partial or extended pediculectomy, mini-hemilaminectomy and hemilaminectomy, with the latter being the most popular approach for the spinal cord (Brisson 2010). The present study provides a rationale to validate surgical approaches with the goal of reducing postoperative pain. In areas with high fiber density, procedures minimizing trauma (mini-hemilaminectomy, pediculectomy, partial or extended pediculectomy) should be favored, as they have been shown to achieve sufficient spinal cord decompression (Braund et al. 1976; Bitetto and Thacher 1986; Black 1988; Jeffery 1988; Brisson 2010).

In humans, persisting or recurring pain after surgery at the site of the lumbo-sacral spine occurs in up to 40 % of patients (Wilkinson 1992). Similar data exist with regard to the dog: 39 % of dogs with IVD herniation show residual deficits after laminectomy (Cudia and Duval 1997), and persisting pain remains in approximately 30 % of patients (Suwankong et al. 2008). An increase in sensory fiber density in the lumbar dura following a laminectomy has been reported in the rat (Saxler et al. 2008) and provides a rationale for persisting or recurring pain after surgery. Preventing dural sensory hyper-innervation, therefore, may contribute to the reduction of low-back pain following spinal surgery (Saxler et al. 2008). To elucidate the role of altered innervation densities in epidural structures after traumatic damage on persisting or recurring back pain, further investigations in affected dogs and comparison with physiological data will be needed.

Sympathetic innervation

Preganglionic sympathetic neurons are nicotinergic cholinergic. As opposed to the situation in humans, however, all the postganglionic sympathetic fibers are aminergic including those innervating effector organs within the soma such as blood vessels or glands. NPY is usually a co-transmitter in noradrenergic postganglionic neurons and may be absent from a subset of sympathetic neurons expressing TH only. Thus, visualizing neurons with NPY alone may constitute an underestimate of the overall sympathetic innervation. NPY has been shown to affect the excitability of sensory nerve fiber endings (Just and Heppelmann 2001). Considering the lack of sympathetic target organs other than blood vessels within the epidural space, NPY-positive adrenergic neurons are likely to represent the most relevant subset.

Our findings provide evidence of putative sympathetic nerve fibers in both the dura mater and the DLL. Unlike Ahmed et al. (1993), who claimed that all sympathetic (i.e., NPY-positive) fibers run independently from blood vessels in the rat dura, our results show that many NPY-positive fibers were closely associated with vessels. In addition to being related to vessels, however, NPY-positive fibers were often associated with CGRP-positive sensory fibers in both the dura and the DLL.

Neuropathic pain and NPY

In addition to arising from nociceptive sensory fibers due to IVD herniation, pain may also arise as a consequence of an immediate neuronal lesion or disease affecting the somatosensory system (Treede et al. 2008). A neuronal lesion triggers the release of different inflammatory mediators and neurotransmitters (Schuh-Hofer and Treede 2012). Through neuroblastic changes, these mediators induce a sensitization of nociceptive neurons and lower the stimulus threshold (Messlinger 1997; Woolf and Costigan 1999; Hucho and Levine 2007; Cheng and Ji 2008; Ji et al. 2009; Schuh-Hofer and Treede 2012). Accordingly, nociceptive fibers may respond to sympathetic efferent activity, which they would not react to under normal conditions (Roberts and Elardo 1985; Tracey et al. 1995b; Schlereth and Birklein 2008).

Treatment of this so-called neuropathic pain has remained a major challenge (Ossipov et al. 2000; Stacey 2005; Eisenberg et al. 2006) and calls for innovative therapeutic approaches. Because our results provide a morphological basis for potential interactions between sympathetic and sensory neurons, they may be of interest to research in current pain treatment concepts that take the sympathetic system into account (Cougnon et al. 1997; Silva et al. 2002; Brumovsky et al. 2007; Hökfelt et al. 2007; Smith et al. 2007).

NPY release in dorsal root ganglia has been reported to affect spinal sensory processing and to be involved in neuropathic pain (Hökfelt et al. 2007). The effects of NPY are described as being pro- or anti-nociceptive, mostly depending on the dose, the receptor type (Y_1, Y_2 receptor) and the site of action (Walker et al. 1988; Tracey et al. 1995b; Abdulla and Smith 1999; Silva et al. 2002; Hökfelt et al. 2007; Smith et al. 2007). In laboratory rodents, the Y_1 and Y_2 receptors have been shown to occur not only in the

central nervous system but also in the peripheral neuronal fibers as well (Tracey et al. 1995b; Zhang et al. 1997; Brumovsky et al. 2005; Brumovsky et al. 2007). Nociception in peripheral neuronal fibers in the skin is modified by NPY and its receptor-agonists and receptor-antagonists, respectively (Tracey et al. 1995a). These authors suggested that a neuronal lesion leads to the upregulation of the density or affinity of NPY receptors or to the amplification of their intracellular effects. Similar to the skin, sympathetic processes may modify pain perception in peripheral sensory fibers in both the dura and the DLL as well. Although we show that sympathetic NPY-positive and sensory CGRP-positive neurons are present in the dura and DLL, further studies will be needed to assess the presence of specific NPY receptors such as Y_1 and Y_2 receptors on neurons in the canine dura and DLL.

Another mechanism of sympathetic pain amplification was recently hypothesized (Tracey et al. 1995a; Perl 1999; Schlereth and Birklein 2008). These authors showed that the expression of α-adrenergic receptors on nociceptive afferents provoked adrenergic sensitization.

Conclusions

In the current study, the presence of extensive innervation is clearly demonstrated in the lateral, dorsal, and ventral canine dura mater and in the DLL. The abundance of CGRP-positive fibers provides strong evidence for sensory innervation of these structures and strongly suggests that low-back pain in the dog may arise from both the dura and the DLL. Taking into account the regional differences in sensory innervation patterns, iatrogenic trauma to intervertebral DLL and lateral dura, especially caudal to T_{13}/L_1 must be expected to entail the most violent pain. Considering the sensory innervation of the dura, efforts to limit hyper-innervation following surgery may contribute to successful pain management. The close proximity of NPY-positive and CGRP-positive fibers is indicative of an interaction between sympathetic and sensory neurons and therefore suggests a possible involvement of sympathetic fibers in pain mediation. Therefore, NPY and its receptors should be taken into account when addressing low-back pain, most notably low-back pain of neuropathic origin.

Acknowledgments The authors express appreciation to Mrs Véronique Gaschen for her untiring laboratory work, Mr Andreas Glarner for his professional preparation work, and Mr Simon König for his excellent photographic work. Further thanks are due to Claudia Spadavecchia. Images were acquired on equipment supported by the Microscopy Imaging Center (MIC) of the University of Bern.

Conflict of interest The authors certify that there was no actual or potential conflict of interest in relation to this article.

References

Abdulla FA, Smith PA (1999) Nerve injury increases an excitatory action of neuropeptide Y and Y2-agonists on dorsal root ganglion neurons. Neuroscience 89:43–60

Ahmed M, Bjurholm A, Kreicbergs A, Schultzberg M (1993) Neuropeptide Y, tyrosine hydroxylase and vasoactive intestinal polypeptide-immunoreactive nerve fibers in the vertebral bodies, discs, dura mater, and spinal ligaments of the rat lumbar spine. Spine 18:268–273

Alanentalo T, Asayesh A, Morrison H, Lorén CE, Holmberg D, Sharpe J, Ahlgren U (2007) Tomographic molecular imaging and 3D quantification within adult mouse organs. Nat Methods 4:31–33

Andres KH, von Düring M, Muszynski K, Schmidt RF (1987) Nerve fibres and their terminals of the dura mater encephali of the rat. Anat Embryol 175:289–301

Andres C, Meyer S, Dina OA, Levine JD, Hucho T (2010) Quantitative automated microscopy (QuAM) elucidates growth factor specific signalling in pain sensitization. Mol Pain 6:98

Arrighi S, Bosi G, Cremonesi F, Domeneghini C (2008) Immunohistochemical study of the pre- and postnatal innervation of the dog lower urinary tract: morphological aspects at the basis of the consolidation of the micturition reflex. Vet Res Commun 32:291–304

Averill S, McMahon SB, Clary DO, Reichardt LF, Priestley JV (1995) Immunocytochemical localization of trkA receptors in chemically identified subgroups of adult rat sensory neurons. Eur J Neurosci 7(7):1484–1494

Bitetto WV, Thacher C (1986) A modified lateral decompressive technique for treatment of canine intervertebral disk disease. J Am Anim Hosp 23:409–413

Black AP (1988) Lateral decompression in the dog: a review of 39 cases. J Small Anim Pract 29:581–588

Boden SD, Davis DO, Dina TS, Patronas NJ, Wiesel SW (1990) Abnormal magnetic-resonance scans of the lumbar spine in asymptomatic subjects. A prospective investigation. J Bone Joint Surg Am 72:403–408

Braund KG, Taylor TK, Ghosh P, Sherwood AA (1976) Lateral spinal decompression in the dog. J Small Anim Pract 17:583–592

Bridge CJ (1959) Innervation of spinal meninges and epidural structures. Anat Rec 133:553–563

Brisson BA (2010) Intervertebral disc disease in dogs. Vet Clin N Am Small Anim Pract 40:829–858

Brumovsky P, Stanic D, Shuster S, Herzog H, Villar M, Hökfelt T (2005) Neuropeptide Y2 receptor protein is present in peptidergic and nonpeptidergic primary sensory neurons of the mouse. J Comp Neurol 489:328–348

Brumovsky P, Shi TS, Landry M, Villar MJ, Hökfelt T (2007) Neuropeptide tyrosine and pain. Trends Pharmacol Sci 28:93–102

Cheng J, Ji R (2008) Intracellular signaling in primary sensory neurons and persistent pain. Neurochem Res 33:1970–1978

Cougnon N, Hudspith MJ, Munglani R (1997) The therapeutic potential of neuropeptide Y in central nervous system disorders with special reference to pain and sympathetically maintained pain. Expert Opin Investig Drugs 6:759–769

Cudia SP, Duval JM (1997) Thoracolumbar intervertebral disk disease in large, nonchondrodystrophic dogs: a retrospective study. J Am Anim Hosp Assoc 33:456–460

Day INM, Thompson RJ (2010) UCHL1 (PGP 9.5): neuronal biomarker and ubiquitin system protein. Prog Neurobiol 90:327–362

Edgar MA, Ghadially JA (1976) Innervation of the lumbar spine. Clin Orthop Relat Res 115:35–41

Edgar MA, Nundy S (1966) Innervation of the spinal dura mater. J Neurol Neurosurg Psychiatry 29:530–534

Eisenberg E, McNicol ED, Carr DB (2006) Efficacy of mu-opioid agonists in the treatment of evoked neuropathic pain: systematic review of randomized controlled trials. Eur J Pain 10:667

Ezaki T, Baluk P, Thurston G, La Barbara A, Woo C, McDonald DM (2001) Time course of endothelial cell proliferation and microvascular remodeling in chronic inflammation. Am J Pathol 158:2043–2055

Forsythe WB, Ghoshal NG (1984) Innervation of the canine thoracolumbar vertebral column. Anat Rec 208:57–63

Giordano A (2005) Regional-dependent increase of sympathetic innervation in rat white adipose tissue during prolonged fasting. J Histochem Cytochem 53:679–687

Groen GJ, Baljet B, Drukker J (1988) The innervation of the spinal dura mater: anatomy and clinical implications. Acta Neurochir (Wien) 92:39–46

Halata Z (1977) The ultrastructure of the sensory nerve endings in the articular capsule of the knee joint of the domestic cat (Ruffini corpuscles and Pacinian corpuscles). J Anat 124:717–729

Higuero AM, Sanchez-Ruiloba L, Doglio LE, Portillo F, Abad-Rodriguez J, Dotti CG, Iglesias T, Higuero AM, Sánchez-Ruiloba L, Doglio LE, Portillo F, Abad-Rodríguez J, Dotti CG, Iglesias T (2010) Kidins220/ARMS modulates the activity of microtubule-regulating proteins and controls neuronal polarity and development. J Biol Chem 285:1343–1357

Hökfelt T, Holets VR, Staines W, Meister B, Melander T, Schalling M, Schultzberg M, Freedman J, Björklund H, Olson L (1986) Coexistence of neuronal messengers–an overview. Prog Brain Res 68:33–70

Hökfelt T, Brumovsky P, Shi T, Pedrazzini T, Villar M (2007) NPY and pain as seen from the histochemical side. Peptides 28:365–372

Hoover DB, Shepherd AV, Southerland EM, Armour JA, Ardell JL (2008) Neurochemical diversity of afferent neurons that transduce sensory signals from dog ventricular myocardium. Auton Neurosci 141:38–45

Hoover DB, Isaacs ER, Jacques F, Hoard JL, Pagé P, Armour JA (2009) Localization of multiple neurotransmitters in surgically derived specimens of human atrial ganglia. Neuroscience 164:1170–1179

Hucho T, Levine JD (2007) Signaling pathways in sensitization: toward a nociceptor cell biology. Neuron 55:365–376

Imai S, Hukuda S, Maeda T (1995) Dually innervating nociceptive networks in the rat lumbar posterior longitudinal ligaments. Spine 20:2086–2092

Jackson P, Thomson VM, Thompson RJ (1985) A comparison of the evolutionary distribution of the two neuroendocrine markers, neurone-specific enolase and protein gene product 9.5. J Neurochem 45:185–190

Jeffery ND (1988) Treatment of acute and chronic thoracolumbar disc disease by mini hemilaminectomy. J Small Anim Pract 29:611–616

Ji R, Gereau RW, Malcangio M, Strichartz GR (2009) MAP kinase and pain. Brain Res Rev 60:135–148

Just S, Heppelmann B (2001) Neuropeptide Y changes the excitability of fine afferent units in the rat knee joint. Br J Pharmacol 132(3):703–708

Kallakuri S, Cavanaugh JM, Blagoev DC (1998) An immunohistochemical study of innervation of lumbar spinal dura and longitudinal ligaments. Spine 23:403–411

Kannari K, Sato O, Maeda T, Iwanaga T, Fujita T (1991) A possible mechanism of mechanoreception in Ruffini endings in the periodontal ligament of hamster incisors. J Comp Neurol 313:368–376

Keller JT, Marfurt CF (1991) Peptidergic and serotoninergic innervation of the rat dura mater. J Comp Neurol 309:515–534

Kojima Y, Maeda T, Arai R, Shichikawa K (1990) Nerve supply to the posterior longitudinal ligament and the intervertebral disc of the rat vertebral column as studied by acetylcholinesterase histochemistry. I. Distribution in the lumbar region. J Anat 169:237–246

Konnai Y, Honda T, Sekiguchi Y, Kikuchi S, Sugiura Y (2000) Sensory innervation of the lumbar dura mater passing through the sympathetic trunk in rats. Spine 25:776–782

Kumar R, Berger RJ, Dunsker SB, Keller JT (1996) Innervation of the spinal dura. Myth or reality? Spine 21:18–26

Lundberg JM, Hökfelt T (1986) Multiple co-existence of peptides and classical transmitters in peripheral autonomic and sensory neurons—functional and pharmacological implications. Prog Brain Res 68:241–262

Macias C, McKee WM, May C, Innes JF (2002) Thoracolumbar disc disease in large dogs: a study of 99 cases. J Small Anim Pract 43:439–446

Messlinger K (1997) Was ist ein Nozizeptor? Schmerz 11:353–366

Mongardi Fantaguzzi C, Thacker M, Chiocchetti R, Furness JB (2009) Identification of neuron types in the submucosal ganglia of the mouse ileum. Cell Tissue Res 336:179–189

Nakamura S, Takahashi K, Takahashi Y, Morinaga T, Shimada Y, Moriya H (1996) Origin of nerves supplying the posterior portion of lumbar intervertebral discs in rats. Spine 21:917–924

Nelson RW, Couto GC (2010) Erkrankungen des Rückenmarks. In: Nelson RW, Couto GC (eds) Innere Medizin der Kleintiere, 2nd edn. Urban & Fischer, München, pp 1106–1131

Ossipov MH, Lai J, Malan TP, Porreca F (2000) Spinal and supraspinal mechanisms of neuropathic pain. Ann N Y Acad Sci 909:12–24

Peleshok JC, Ribeiro-da-Silva A (2011) Delayed reinnervation by nonpeptidergic nociceptive afferents of the glabrous skin of the rat hindpaw in a neuropathic pain model. J Comp Neurol 519:49–63

Perl ER (1999) Causalgia, pathological pain, and adrenergic receptors. Proc Natl Acad Sci USA 96:7664–7667

Portmann-Lanz CB, Schoeberlein A, Portmann R, Mohr S, Rollini P, Sager R, Surbek DV (2010) Turning placenta into brain: placental mesenchymal stem cells differentiate into neurons and oligodendrocytes. Am J Obstet Gynecol 202:294.e1–294.e11

Roberts WJ, Elardo SM (1985) Sympathetic activation of A-delta nociceptors. Somatosens Res 3:33–44

Rosenfeld MG, Mermod JJ, Amara SG, Swanson LW, Sawchenko PE, Rivier J, Vale WW, Evans RM (1983) Production of a novel neuropeptide encoded by the calcitonin gene via tissue-specific RNA processing. Nature 304:129–135

Roudenok V (2000) Changes in the expression of neuropeptide Y (NPY) during maturation of human sympathetic ganglionic neurons: correlations with tyrosine hydroxylase immunoreactivity. Ann Anat 182(6):515–519

Russo D, Clavenzani P, Sorteni C, Bo Minelli L, Botti M, Gazza F, Panu R, Ragionieri L, Chiocchetti R (2013) Neurochemical features of boar lumbosacral dorsal root ganglion neurons and characterization of sensory neurons innervating the urinary bladder trigone. J Comp Neurol 521(2):342–366

Saxler G, Brankamp J, Knoch M, Löer F, Hilken G, Hanesch U (2008) The density of nociceptive SP- and CGRP-immunopositive nerve fibers in the dura mater lumbalis of rats is enhanced after laminectomy, even after application of autologous fat grafts. Eur Spine J 17:1362–1372

Schlereth T, Birklein F (2008) The sympathetic nervous system and pain. NeuroMol Med 10:141–147

Schuh-Hofer S, Treede RD (2012) Definition und Pathophysiologie neuropathischer Schmerzen. Nervenheilkunde 3:115–122

Sekiguchi Y, Konnai Y, Kikuchi S, Sugiura Y (1996) An anatomic study of neuropeptide immunoreactivities in the lumbar dura mater after lumbar sympathectomy. Spine 21:925–930

Silva AP, Cavadas C, Grouzmann E (2002) Neuropeptide Y and its receptors as potential therapeutic drug targets. Clin Chim Acta 326:3–25

Simpson ST (1992) Intervertebral disc disease. Vet Clin N Am Small Anim Pract 22:889–897

Smith PA, Moran TD, Abdulla F, Tumber KK, Taylor BK (2007) Spinal mechanisms of NPY analgesia. Peptides 28:464–474

Stacey BR (2005) Management of peripheral neuropathic pain. Am J Phys Med Rehabil 84:S4–S16

Stoffel MH (2011) Funktionelle Neuroanatomie für die Tiermedizin: Somatisches Nervensystem und höhere Sinne. Enke, Stuttgart, pp 122–215

Suwankong N, Meij BP, Voorhout G, de Boer AH, Hazewinkel HAW (2008) Review and retrospective analysis of degenerative lumbosacral stenosis in 156 dogs treated by dorsal laminectomy. Vet Comp Orthop Traumatol 21:285–293

Tracey DJ, Cunningham JE, Romm MA (1995a) Peripheral hyperalgesia in experimental neuropathy: mediation by alpha 2-adrenoreceptors on post-ganglionic sympathetic terminals. Pain 60:317–327

Tracey DJ, Romm MA, Yao NN (1995b) Peripheral hyperalgesia in experimental neuropathy: exacerbation by neuropeptide Y. Brain Res 669:245–254

Treede R, Jensen TS, Campbell JN, Cruccu G, Dostrovsky JO, Griffin JW, Hansson P, Hughes R, Nurmikko T, Serra J (2008) Neuropathic pain: redefinition and a grading system for clinical and research purposes. Neurology 70:1630–1635

Tropel P, Platet N, Platel J, Noël D, Albrieux M, Benabid A, Berger F (2006) Functional neuronal differentiation of bone marrow-derived mesenchymal stem cells. Stem Cells 24:2868–2876

Wakisaka S, Kajander KC, Bennett GJ (1991) Increased neuropeptide Y (NPY)-like immunoreactivity in rat sensory neurons following peripheral axotomy. Neurosci Lett 124:200–203

Walker MW, Ewald DA, Perney TM, Miller RJ (1988) Neuropeptide Y modulates neurotransmitter release and Ca2+ currents in rat sensory neurons. J Neurosci 8:2438–2446

Wilkinson HA (1992) The failed back syndrome: the role of improper surgery in the etiology of the failed back syndrome, 2nd edn. Springer, New York

Willenegger S, Friess AE, Lang J, Stoffel MH (2005) Immunohistochemical demonstration of lumbar intervertebral disc innervation in the dog. Anat Histol Embryol 34:123–128

Wilson PO, Barber PC, Hamid QA, Power BF, Dhillon AP, Rode J, Day IN, Thompson RJ, Polak JM (1988) The immunolocalization of protein gene product 9.5 using rabbit polyclonal and mouse monoclonal antibodies. Br J Exp Pathol 69:91–104

Wong HC, Taché Y, Lloyd KC, Yang H, Sternini C, Holzer P, Walsh JH (1993) Monoclonal antibody to rat alpha-CGRP: production, characterization, and in vivo immunoneutralization activity. Hybridoma 12:93–106

Woolf CJ, Costigan M (1999) Transcriptional and posttranslational plasticity and the generation of inflammatory pain. Proc Natl Acad Sci USA 96:7723–7730

Yamada H, Honda T, Kikuchi S, Sugiura Y, 1524 (1998) Direct innervation of sensory fibers from the dorsal root ganglion of the cervical dura mater of rats. Spine 23:1524–1529 (discussion 1529–1530)

Yamada H, Honda T, Yaginuma H, Kikuchi S, Sugiura Y (2001) Comparison of sensory and sympathetic innervation of the dura mater and posterior longitudinal ligament in the cervical spine after removal of the stellate ganglion. J Comp Neurol 434:86–100

Zhang X, Shi T, Holmberg K, Landry M, Huang W, Xiao H, Ju G, Hökfelt T (1997) Expression and regulation of the neuropeptide Y Y2 receptor in sensory and autonomic ganglia. Proc Natl Acad Sci USA 94:729–734